Proceedings of the 6th International Conference on Gas Hydrates (ICGH 2008),
Vancouver, British Columbia, CANADA, July 6-10, 2008.

SEISMIC REFLECTION BLANK ZONES IN THE ULLEUNG BASIN, OFFSHORE KOREA, ASSOCIATED WITH HIGH CONCENTRATIONS OF GAS HYDRATE

Iulia Stoian*
Department of Earth and Ocean Sciences
University of Victoria
3800 Finnerty Road, Victoria, BC, V8P 5C2
CANADA

Keun-Pil Park, Dong-Geun Yoo
30 Gajeongdong, Yuseong-gu, Daejeon
KOREA

R. Ross Haacke, Roy D. Hyndman
Geological Survey of Canada
Pacific Geoscience Center
9860 West Saanich Road, Sindey, BC, V8L 4B2
CANADA

Michael Riedel
Earth and Planetary Sciences
McGill University
3450 University St., Montreal, QC, H3A 2A7
CANADA

George D. Spence
Department of Earth and Ocean Sciences
University of Victoria
3800 Finnerty Road, Victoria, BC, V8P 5C2
CANADA

ABSTRACT

It has recently been recognized that abundant gas hydrates occur in localized zones of upwelling fluids, with concentrations much higher than in regional distributions associated with bottom-simulating reflectors (BSRs). We report a study of multi-channel seismic reflection data across such structures in the Ulleung Basin, East Sea backarc offshore Korea, an area with few BSRs. The structures are commonly up to several km across and a few hundred meters in depth extent, and are characterized by reduced reflectivity and bowed-up sediment reflectors on time-migrated sections. The seismic pull-up mainly results from higher velocities, although physical deformation due to folding and faulting is not ruled out. Some of the features extend upward close to the seafloor and others only partway through the gas hydrate stability zone. The base of gas hydrate stability zone (BGHSZ), calculated assuming a regional average constant heat flow of 110 mW/m^2, is confirmed by the presence of gas inferred from reduced instantaneous frequencies and high instantaneous amplitudes, and from a decrease in seismic velocities. The

* Corresponding author: Phone: +1 250 721 6188 Fax +1 250 472 4620 E-mail: istoian@uvic.ca

vents are fed by upward migrating free gas or gas-rich fluids through near-vertical conduits probably due to regional, upward fluid flow caused by tectonic compression of the basin.

Keywords: gas hydrates, blank zones, seismic velocity, base of gas hydrate stability, heat flow

INTRODUCTION

Acoustically blank zones with pulled-up reflectors, also known as chimneys or cold vents, are believed to host large concentrations of gas hydrate in some deep-sea regions. IODP Leg 311 drilled one such structure on Northern Cascadia, where very large concentrations of hydrate were found in a 40 m thick region below the seafloor [1]. Numerous blank zones have been identified in the Ulleung Basin offshore Korea on seismic profiles [2].

An extensive high quality multi-channel seismic survey of the Ulleung Basin has been carried out by KIGAM (Korea Institute of Geoscience and Mineral Resources). The multi-channel seismic data discussed in this paper are from the central part of the Ulleung Basin, offshore Korea. This paper discusses the methods applied to the data to infer indications of gas hydrate and determine its concentration. Some of the most important results are shown and interpreted. The focus is seismic velocity, which is the best seismic indicator for the presence of gas hydrate and free gas. Higher velocities above the base of gas hydrate stability zone (BGHSZ) indicate gas hydrate and lower velocities below the BGHSZ free gas. Seismic velocities higher than a no-hydrate velocity-depth reference can be used to estimate gas hydrate concentrations. A limit for the BGHSZ is estimated from regional heat flow calculated from the depth of the bottom-simulating reflector (BSR) identified on several seismic profiles in the basin. Seismic attributes are calculated to see whether the presence of gas can be detected. Haacke et al. [3] present related results from a different seismic line using some of the methods described in this paper.

SEISMIC DATA AND PROCESSING

The 2D multi-channel seismic data were acquired using an airgun source of 1000 in^3 and 240 recording channels by KIGAM. The near offset is 161 m and the far offset is 3149 m, with a receiver spacing of 12.5 m. The distance between shots is 25 m, which results in a CDP spacing of 6.25 m. The sampling rate is 1 ms, with a dominant frequency of 70 Hz.

A time migrated seismic section is shown in Fig. 1. The top 250 ms imaged by the data is represented by turbidites and hemipelagic sediments, that appear as relatively continuous reflectors, and debris flow deposits which have a chaotic character. Turbidites and mass transport complexes can be identified below the top 250 ms, by their structureless character, short reflectors and near transparent zones.

A few structures with reduced reflection amplitudes and pulled-up reflectors can be identified from these data and are subject to further analysis. These structures have the appearance of chimneys on large vertical exaggeration seismic sections but not on true scale (Fig. 2): they are typically 200 m in depth extent and over 500 m wide.

The seismic processing is done using the Globe Claritas software. A Butterworth band-pass filter with corner frequencies 5-15-150-250 Hz is applied to the shots, followed by spherical divergence and deconvolution. The data are sorted to CDPs, and normal and dip moveout are done using a preliminary velocity. A more detailed velocity analysis is then carried out using semblance spectra. Stacking velocity profiles are picked at a fixed increment of 50 CDPs (300 m) with tighter spacing of 10 CDPs (60 m) in the blank zones. The velocities are checked by looking at the normal-moveout-corrected CDP gathers to see if the reflectors are flattened and are adjusted if necessary. The stacking velocities are smoothed, converted to interval velocities using the Dix equation [4], spatially smoothed and used in the finite difference migration of the stacked data.

Stacking velocity results

The stacking velocities are gridded using a near-neighbor algorithm and shown in Fig. 3, where the crosses indicate the location of the input data. The blank zones are separated by the dashed lines. There are some positive velocity anomalies above the BGHSZ in the features located around CDPs 3400-3500, both positive and negative anomalies around the depth of the BGHSZ for the features at CDP 2000 and CDP 6000.

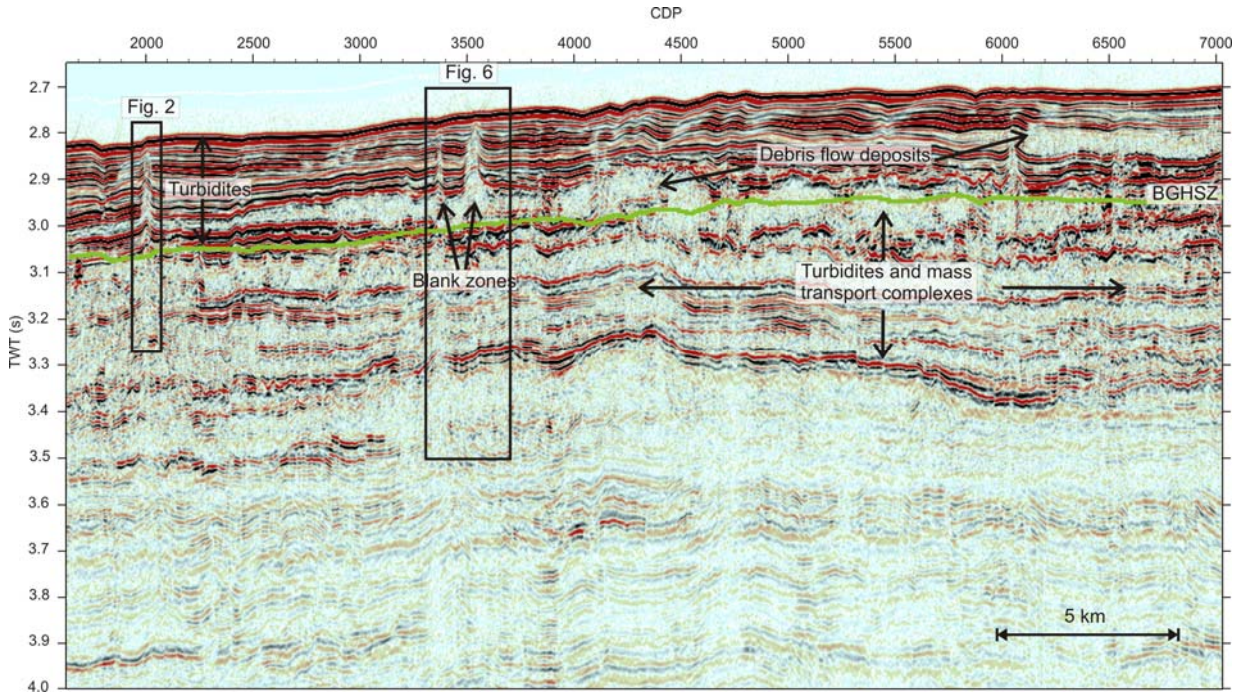

Figure 1. Time migrated section from multi-channel seismic data. The most significant features are the blank zones that have reduced amplitudes and pulled-up reflectors found in turbidite layers. BGHSZ: Base of gas hydrate stability zone calculated for a heat flow of 110 mW/m^2. The locations of the structures shown in Fig. 2 and Fig. 6 are indicated by the boxes.

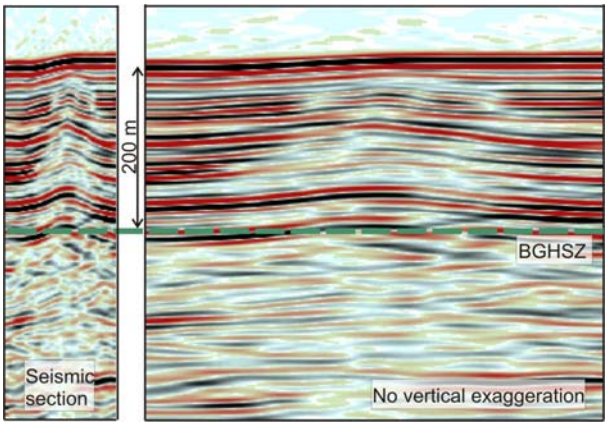

Figure 2. Blank zone from seismic line shown in Fig. 1; comparison between the chimney-like appearance in the seismic section (left) and its true scale (right).

The velocity picks are separated into regions outside and inside the blank zones and the seafloor is adjusted to zero depth. All picks within a given region are averaged horizontally and a vertical running mean is calculated every 5 ms on windows of 40 ms. The results are shown in Fig. 4, together with one standard deviation from the mean. Outside the blank zones, velocities increase by about 2 m/s in the top 150 ms and by in about 5 m/s from 150 ms to 200 ms. Velocity is relatively constant between 200 and 300 ms, followed by a relatively uniform increase with depth. Within the blank zones, the velocities are 2-3 m/s lower from 75 to 175 ms, 3-5 m/s higher from 175 to 275 ms and about 5 m/s lower from 300-350 ms as compared to areas outside. Outside the blank zones, the standard deviation for velocity ranges from about 2 m/s close to the seafloor to 10 m/s at 500 ms bsf; the standard deviation is about 3 m/s larger for velocities inside the blank zones. The semblance analysis inside the blank zones involves a greater level of uncertainty because of the low amplitudes used to calculate the semblance. Additionally, no velocity can be picked for certain reflectors, for which direct comparisons with areas outside cannot be made.

Interpretation of velocity results

An increase in velocity of 5 m/s outside blank zones and 8-10 m/s inside blank zones at about 175 ms bsf marks the limit between the turbidities above and the debris flows below. This increase and the higher velocities between 175 and 250 ms inside the blank zones could also be a result of the presence of gas hydrate above the BGHSZ. The abrupt decrease of 8 m/s in velocities inside the blank zones from 250 to 375 ms can be attributed

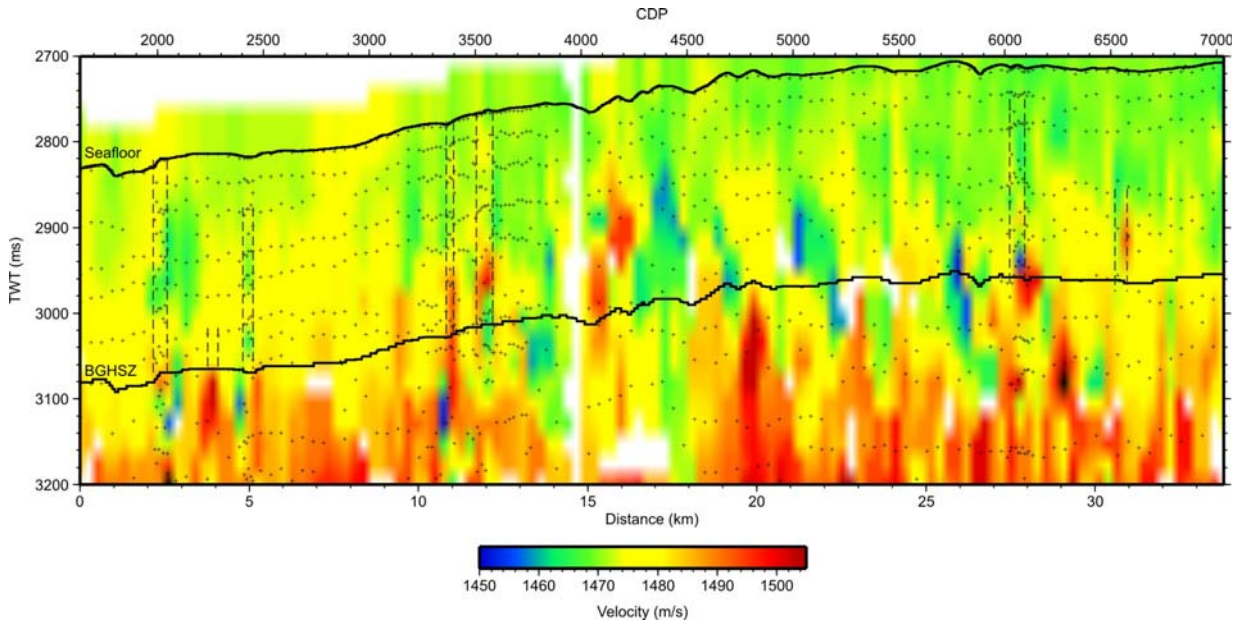

Figure 3. Gridded stacking velocities obtained by semblance analysis from data shown in Fig. 2. The crosses represent the calculated data points. The extent of the blank zones is shown by the dashed vertical lines.

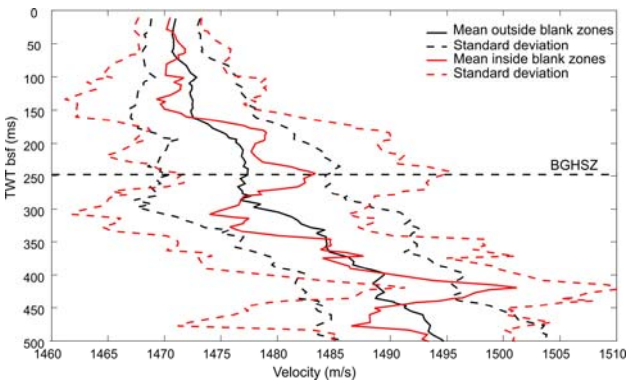

Figure 4. Running mean of the data shown in Fig. 3, calculated separately for the blank zones (red curve) and areas outside them (black curve). The mean plus/minus one standard deviation are shown by the dashed curves. The mean is calculated using a 40 ms long running window in 5 ms increments.

to the presence of gas, since the BGHSZ, estimated from heat flow, corresponds to a time of 250 ms bsf (Fig. 4). The velocity outside the blank zones is constant between 200 and 300 ms, which implies a decrease in interval velocity, so it could as well result from the presence of gas.

The velocity anomalies inside the blank zones are within one standard deviation; however, the anomalies are thought to be meaningful since it is very likely that part of the standard deviation is also due to lateral variability in velocities along the 33 km long profile.

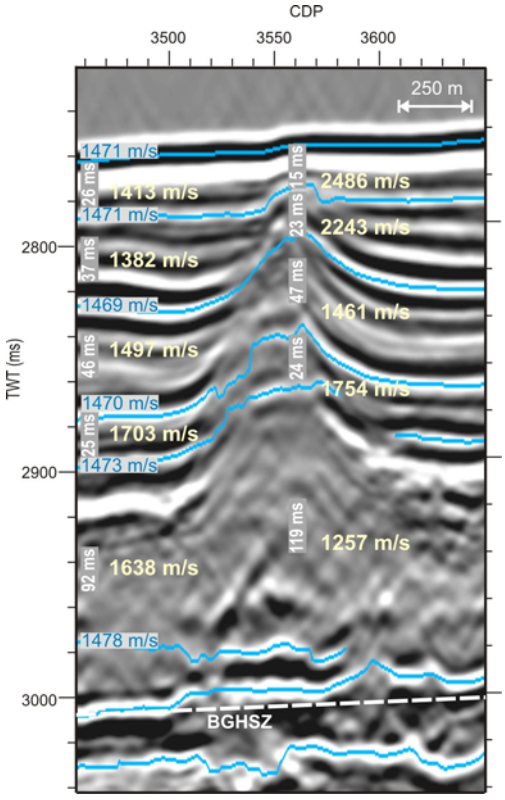

Figure 5. Interval velocities inside the blank zone, calculated under the assumption that the reflectors are physically flat, so the pull-up is only a result of high velocities. The velocities are calculated from the interval velocities derived using the Dix equation from the area next to the blank zone.

Regularized velocity inversion

The interval velocities determined using the Dix equation have unrealistic values and large uncertainties for small variations in stacking velocities, for thin layers and where the velocity increases slightly over a thick interval. Also, the Dix equation only works for an increasing velocity function.

The Dix equation is solved by inverse methods using regularization, which gives more realistic values and uncertainties for the interval velocities.

The Dix equation is expressed by a linear relationship between the squared RMS velocity and squared interval velocity. The RMS velocity is approximated by the stacking velocities obtained from the semblance analysis.

The regularized solution is obtained by setting up two goals: first is to minimize the data misfit in a least squares sense and the second is to have a smooth interval velocity function. In this way, the interval velocities estimated do not have wild variations. This is achieved by using different regularization schemes, depending on the type of solution desired - smallest, flattest [5] or smoothest [6]. The relative importance of the two goals is achieved by a regularization parameter. In this case, the interval velocity uncertainties are derived from the uncertainties of RMS velocities.

The non-linear problem is investigated by taking into account errors on the time of the reflectors corresponding to the RMS velocities, to determine numerically how the errors influence the solution. An analytical solution of this problem, showing that the time error is not significant, is given by Hajnal and Sereda [7].

BASE OF GAS HYDRATE STABILITY ZONE FROM HEAT FLOW

The heat flow is first calculated from the depth of the BSR identified on several seismic lines, other than the one discussed here, where no BSR can be identified. The values for the heat flow calculated using a simple conductive model, range from 90 to 130 mW/m^2. The values are slightly larger than the average heat flow measured in this area [8].

A hydrostatic increase in pressure is assumed and the phase boundary condition relating the pressure and temperature at the BGHSZ is taken from Bouriak et al. [9]. The thermal conductivity is calculated as a function of depth using an empirical equation from Davis et al. [10]. The depth for the BGHSZ is predicted for the data discussed in this paper using a constant heat flow of 110 mW/m^2.

BLANK ZONES ANALYSES

Interval velocity from pulled-up reflectors

The reflectors in the blank zones are bowed up in time sections. The pull-up could result from a combination of higher velocity, physical bowing of reflectors and structural deformation resulting from folds and faults.

Interval velocities are calculated inside the blank zone centered at CDP 3550 under the assumption that there is no physical bowing of reflectors, i.e., the distance between reflectors is the same both outside and inside the blank zones, so the pull-up is only a velocity effect. The velocity in each layer in the blank zones (Fig. 5) is calculated as a product of the velocity corresponding to the same layer outside the blank zone and the ratio between the interval thickness (in ms) outside to interval thickness inside the blank zone. The calculations assume vertical incidence of rays, and use the outside velocity as a reference for a normally increasing velocity trend.

High velocities of about 2500 m/s and 2250 m/s are calculated in the top two layers, and a low velocity of 1250 m/s is required to explain the thickness of the layer from 2900 to 2980 ms. The largest increase in the pull-up is for the reflectors close to the seafloor, and the reflectors below have only an apparent pull-up, resulting from above.

Interpretation of velocity

The velocities derived from seismic pull-up would imply 40-50 % gas hydrate concentration in the pore space in the top two layers for sediments with porosity of 50 % using the Lee et al. [11] weighted equation. The velocities would be lower if some physical upward bending is considered to cause the pull-up.

It is useful to compare the interval velocities from pull-up with those derived directly from RMS velocities. Due to the low reflection amplitudes inside the blank zone, only a few RMS velocities could be obtained for the first two reflectors below the seafloor, so a direct comparison is not easily possible. The velocities for the next reflectors in the blank zone are 5-10 m/s higher than outside (Fig. 3), resulting in higher interval velocities.

Seismic attributes

Instantaneous amplitudes and frequencies are computed from the migrated stack from CDP 3300 to CDP 3700 shown in Fig. 6a. Two blank zones are present in this area, indicated by the green and red boxes, separated from the area outside them in the black box. To reduce the noise in the attributes, especially in the case of instantaneous frequency, the attributes are averaged using a running vertical window of 25 ms and a horizontal window of 5 CDPs (33 m). Three distinct zones are considered for comparison: the two blank zones and the area outside. The instantaneous amplitude and frequency values for each CDP trace are then added over the distance indicated by the colored boxes, as shown in Fig. 6b and 6c.

The amplitude inside both features (green and red) is reduced above the BGHSZ as compared to the area outside. The reflectors at 3025 ms and 3275 ms have high amplitudes in the red and black zones. A decrease in frequency is seen immediately below these reflectors. The amplitude in the green zone is low everywhere above and below the BGHSZ, whereas the amplitude in the red zone is reduced only above the BGHSZ.

Interpretation of seismic attributes

The reduction in frequency in the red and black zone below the reflectors at 3025 ms and 3275 ms, associated with the increase in amplitudes at these times imply the presence of gas below these reflectors. In the red zone, amplitudes at the 3275 ms reflector and frequencies above this reflector are high, as compared to reduced amplitudes above 3025 ms and reduced frequencies immediately below.

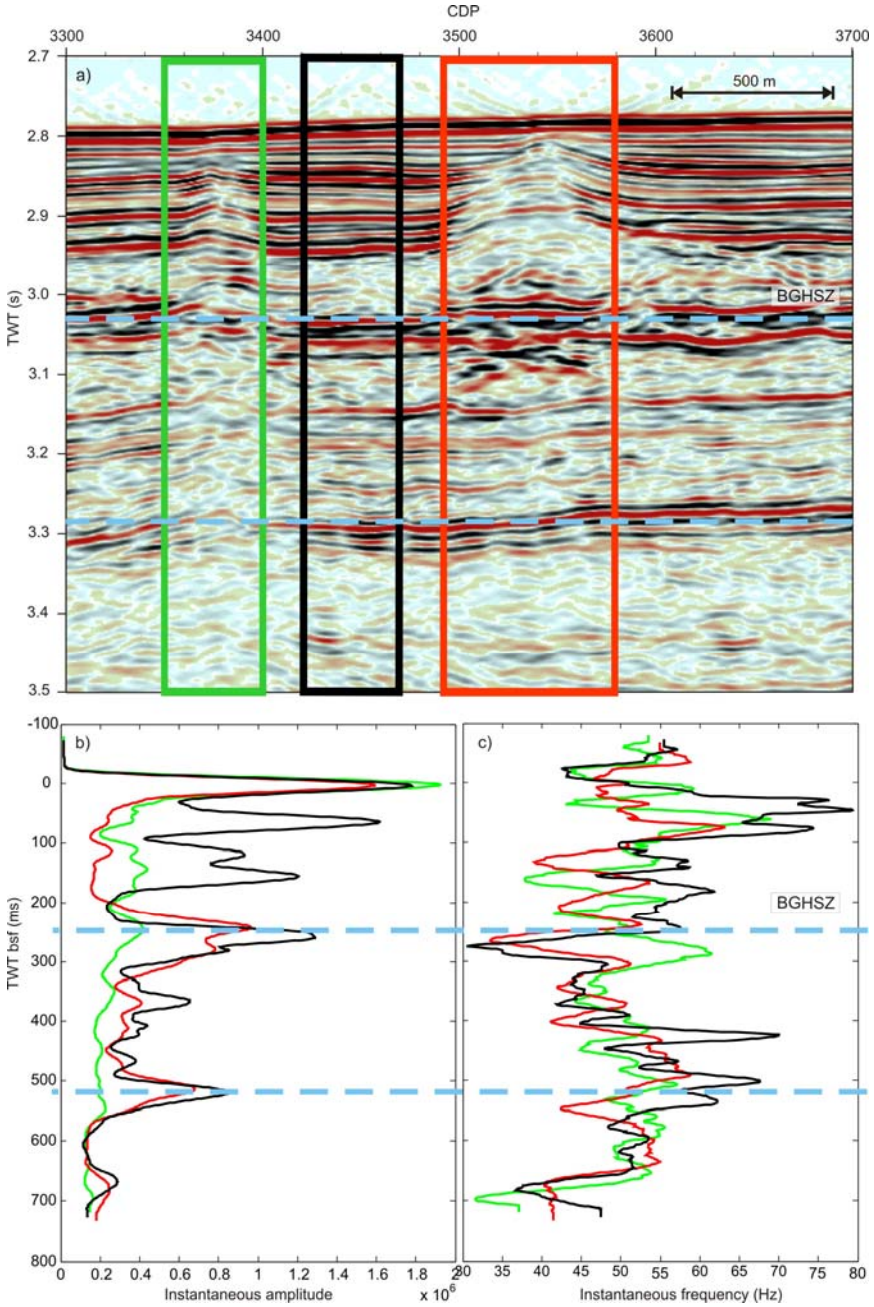

Figure 6. a) A section of interest from the seismic line in Fig. 1, showing two blank zones. Instantaneous amplitude (b) and instantaneous frequency (c) computed from the seismic data separately for the three zones. The blank zones are indicated by the green and red boxes, the area outside them by the black box (a) and the averages of the attributes from each zone (first averaged with a vertical running window of 25 ms and horizontal window of 5 CDPs (33 m)) are shown by the corresponding color curves in b) and c).

This implies that the sediments above the BGHSZ do not attenuate the energy, and the reduction in amplitude is due to the low reflectivity of the reflectors.

The reduced amplitudes and frequencies in the green zone above and below the BGHSZ with the exception of an anomalous increase in frequency below the BGHSZ, suggest the presence of gas migrating upwards to feed the blank zone above and possibly move laterally to feed the blank zone on the right. The gas is not trapped anywhere in the blank zone, since it does not produce any response similar to the one for the black and red zones. Our limitation is that we only have a 2D dataset, so it is possible that some of the rays are coming from the sides of the features.

CONCLUSIONS

Numerous blank zones that contain significant concentrations of gas hydrate have been identified from multi-channel seismic data in the Ulleung Basin, offshore Korea. The presence of gas hydrate is inferred from high velocities derived from semblance analysis and from the apparent pull-up of the reflectors. The stacking velocities are more uncertain in the blank zones, but they point to anomalous velocities: higher velocities in a region of 100 ms above the BGHSZ and lower velocities below as compared to areas outside, implying the presence of gas hydrate and gas, respectively. The stacking velocities outside the blank zones appear almost constant in a region 100 ms thick around the BGHSZ, which implies a decrease in interval velocity. We seek to overcome the problem of unrealistic interval velocities calculated using the Dix equation, by constraining them using different regularization methods.

The depth of the BGHSZ predicted using a constant heat flow estimate of 110 mW/m^2 is confirmed by the inferred presence of gas from a drop in the instantaneous frequency, sometimes associated with high amplitudes.

Geological Survey of Canada Publication 20080034.

REFERENCES

[1] Riedel M, Collett TS, Malone MJ, and the expedition 311 scientists, 2006. *Proceedings of the Integrated Ocean Drilling Program, 311*: Washington, DC, doi:10.2204/iodp.proc.311.101. 2006.

[2] Lee JH, Baek YS, Ryu BJ, Riedel M, Hyndman RD. *A seismic survey to detect natural gas hydrate in the East Sea of Korea.* Marine Geophys. Res. 2005; 26: 51-59.

[3] Haacke RR, Park K-P, Stoian I, Hyndman RD, Schmidt U. *High-flux gas venting in the East Sea, Korea, from analysis of 2D seismic reflection data*. Proceedings of the 6th International Conference on Gas Hydrates, 2008, this volume.

[4] Dix CD, *Seismic velocities from surface measurements.* Geophysics 1955; 20: 8-86.

[5] Oldenburg DW, Levy S, Stinson K, *Root-mean-square velocities and recovery of the acoustic impedance*. Geophysics 1984; 49: 1653-1663.

[6] DuBose JB, *A technique for stabilizing interval velocities from the Dix equation*. Geophysics 1988; 53: 1241-1243.

[7] Hajnal Z, Sereda IT, *Maximum uncertainty of interval velocity estimates*. Geophysics 1981; 46: 1543-1547.

[8] International Heat Flow Commission, Global Heat Flow Data Set http://www.geo.lsa.umich.edu/IHFC/heatflow.html

[9] Bouriak S, Vanneste M, Saoutkine A. *Inferred gas hydrates and clay diapirs near the Storegga Slide on the southern edge of the Vøring Plateau*. Marine Geology 2000; 163: 125-148.

[10] Davis EE, Hyndman RD, Villinger H. *Rates of fluid expulsion across the northern Cascadia accretionay prism: constraints from new heat flow and multichannel seismic reflection data*. J. Geophys. Res. 1990; 95: 8869-8889.

[11] Lee MW, Hutchinson, DR, Collett, TS, Dillon, WP, *Seismic velocities for hydrate-bearing sediments using weighted equation*. J. Geophys. Res. 1996; 101:20,347-20,358.